11^{th} International Conference on Fracture Mechanics of Concrete and Concrete Structures
FraMCoS-11
J. M. Chandra Kishen, A. Ramaswamy, S. Ray and R. Vidyasagar (Eds)
https://doi.org/10.21012/FC11.0923110

EFFECT OF NOTCH SIZE ON THE FRACTURE BEHAVIOUR OF CONCRETE

Yogesh R*, J M Chandra Kishen†

* † Department of Civil Engineering
Indian Institute of Science
Bangalore, India, 560012
e-mail *: yogeshr@iisc.ac.in
e-mail†: chandrak@iisc.ac.in

Key words: Wedge splitting test (WST), Acoustic emission (AE), Digital image correlation (DIC), micro cracking, Fracture, Fracture process zone

Abstract. Concrete is a quasi-brittle material exhibiting low strength under tension. The presence of a notch or crack can significantly reduce the material's fracture properties due to stress concentration at the notch tip and the formation of the fracture process zone (FPZ). In the FPZ, microcracks are formed which coalesce to form macrocracks and eventually leading to failure. Existing literature shows that the size of pre-existing notch in concrete can significantly affect the strength and cracking behaviour. In order to study the effect of the notch size on the fracture behaviour of plain concrete, a series of wedge-splitting tests (WST) are conducted on specimens with different notch-to-depth ratios. Using acoustic emission (AE) and digital image correlation (DIC) methods, the fracture characteristics of concrete specimens with various notch sizes are studied. Throughout the loading process, AE measurements are employed to capture the acoustic emission events, providing details on the position and time of crack initiation and propagation. The crack mouth opening displacement (CMOD) and crack tip opening displacement (CTOD) of the specimens are calculated using DIC measurements to examine the deformation and strain fields on the surface. The findings reveal that, with increasing notch size, the size dependent fracture energy of concrete decreases. The AE analysis demonstrates that there is not much change in the number of events or acoustic energy with change in notch depth, indicating that the mechanisms of fracture remains the same irrespective of the notch size.

1 Introduction

In order to ensure durability and greater lifespan, it is important to thoroughly investigate a variety of factors while designing concrete structures. These include quality of concrete mix, quantity of reinforcement, curing techniques, moisture control and waterproofing, and crack control. However, if structures have been in use for a long time or have undergone a lot of stress, damage or cracks are inevitably caused. This reduces the concrete's mechanical strength, which directly affects the dependability and longevity of the structures and may even result in catastrophic failures. Understanding concrete's fracture behaviour is crucial to prevent extensive spread of damage. The main reason for concrete fracture is the development of tensile cracks, as concrete is weak in tension. During the analysis and design of the structures, pre-existence defects such as cracks, voids, flaws due to the inhomogenity of the material are considered. These cracks may be external or internal. When the structure is exposed to external loads, these cracks act as stress rais-

ers and propagate. Based on the maximum principal stress theory, the cracks propagate perpendicular to the direction of applied load (either tensile load or compressive load), when the tensile stress exceeds its allowable value.

The notch or crack can significantly reduce the material's fracture properties due to stress concentration at the notch tip and the formation of the fracture process zone (FPZ). The wedge splitting specimen behaviour is studied by several researches [3, 6, 8, 9] to determine the fracture characteristics. The size effect on wedge splitting test was conducted by Bakour and Ftima [8]. The micromechanical properties using acoustic emission and image processing of beams are carried out by Keertana and Kishen [5], Bhowmik and Ray [4]. A similar study on wedge splitting specimens was carried out by and Singh et al. [9]. Bažant [2] explained the importance of size indepedent fracture energy to characterize cracking in concrete. In most of the fracture experiments, notched specimens are used. Different notch sizes are used on various tests as reported in the literature. Studies related to the effect of notch size on the fracture properties on concrete are limited. While designing the geometrical properties of the notched specimens under fatigue loading, it is very useful to know apriori the effect of the notch size on the failure characteristics of the material.

In this study, quasi-static tests of concrete wedge splitting specimens with pre-existing notch of three different sizes under monotonically increasing crack opening displacement are conducted. With the use of digital image processing and acoustic emission, the concrete's fracture behaviour is quantified. Estimates of the mechanical and fracture parameters and a description of the fracture phenomenon are provided.

2 Experimental setup and testing of specimens

This section comprises information about specimen sizes, a detailed description of the material used in the experiment, and an account of the experimental research conducted.

2.1 Materials used and preparation of the specimens

Wedge splitting concrete specimen (WSP) are prepared using Portland cement that complies with IS 1489 Part 1 [1991]. Fine aggregate of river sand within the confines of zone III as defined by IS 2386 (Part I) [1963], and coarse aggregate of crushed stone aggregates with a maximum size D_{max} of 12.5mm are used to prepare the concrete. Mix design is done as per IS 10626-2019. The water-cement ratio is fixed as 0.55, and the ratio of cement: fine aggregate: coarse aggregate is 1:2.30:2.70. Once the mix had been refined, the concrete specimens were prepared. Three sets of concrete specimens are prepared, each with a notch to depth ratio of 0.20, 0.35, and 0.50. The specimens measure 300 mm in length, 300 mm in height, and 100 mm in thickness with the dimension (in mm) show in Figures 1 to 3. Three cubes and three cylinders were also casted along with the test specimens to obtain the compressive and splitting tensile strength. All specimens are taken out of the mould after a day and immersed in water tanks to cure for twenty eight days. The mean and standard deviation of elastic properties are shown in Table 1.

Table 1: Details of Mechanical properties (cubes and cylinders)

Properties	Mean	σ
Compressive strength, f_{ck} (MPa)	48.00	3.45
Splitting tensile strength, f_{sp} (MPa)	3.36	0.21
Modulus of elasticity, E, (MPa)	34205	2155

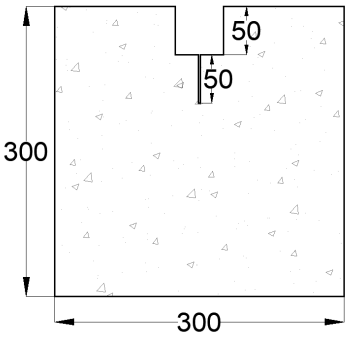

Figure 1: a/D:0.20

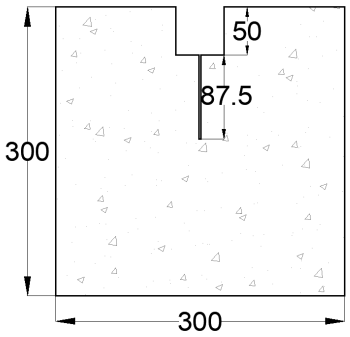

Figure 2: a/D:0.35

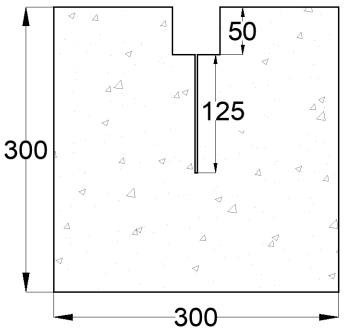

Figure 3: a/D:0.50

Figure 4: Geometric details of specimen with different a/d ratio (all dimensions in mm)

2.2 Experimental setup

A 35kN capacity digitally controlled servo-hydraulic machine is used to test the wedge-splitting specimens. At the top of specimen, close to the notch, steel plates with bevelled edges are fixed to mount the CMOD gauge. The wedge splitting fixture is attached to the specimen and fixed to the top crosshead of the machine. The bottom of the specimen rests on a roller support. The loading configuration and experimental setup are shown in Figure 5. The experiment is carried out under CMOD control at a loading rate of 0.001mm/s. The data acquisition system acquired the data on time, load (in kN), and CMOD (in mm).

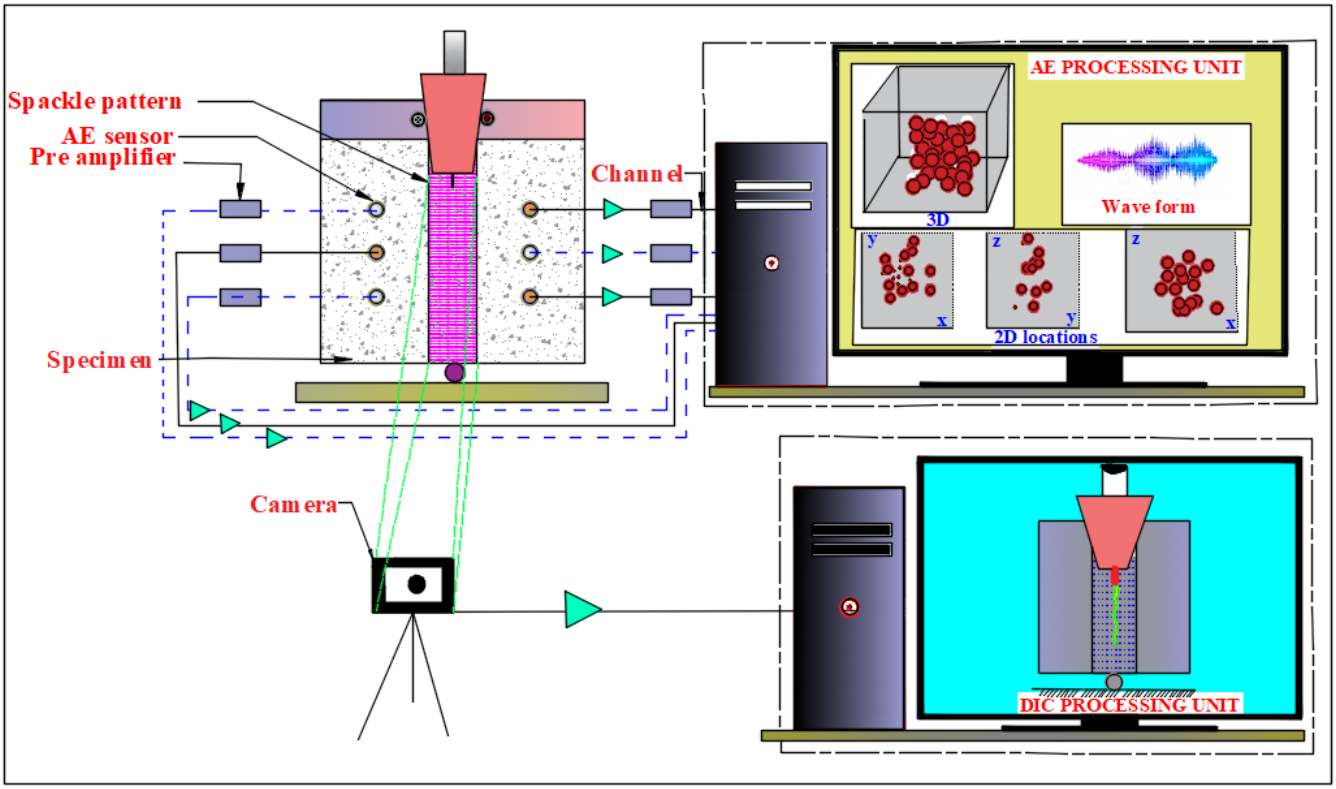

Figure 5: Schematic representation of the experimental set-up

Figure 6 depicts the loading and schematic diagram of the specimen and CMOD gauge. The wedge angle of the wedging device is $\alpha = 15^0$. The wedging device, transfers the vertical load to the rollers by wedge action as indicated in the figure 6. The force that is transmitted in a horizontal direction is marked as F_{SH}. Based on the force equilibration in the horizontal direction. The splitting tensile force, F_{SH}, is determined by Equation 1,

$$F_{SH} = \frac{F_v}{2tan(\alpha)} = \frac{F_v}{2tan(15^0)} = 1.85F_v \quad (1)$$

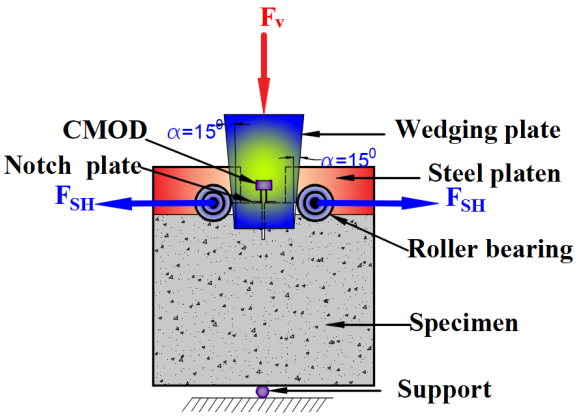

Figure 6: Specimen with wedge splitting device

2.3 Details of acoustic emission and digital image processing

The AE system is used to capture the elastic waves generated inside the specimen when it is loaded. It consists of AE sensors, preamplifiers, and data acquisition system. The sensors are of piezo-electric type with a resonating frequency of 50Hz (RD50). They capture the signals from the specimen, convertes them to electrical signals and pass them onto the preamplifier. The preamplifier amplifies the electrical signal and sends them to the data acquisition system. A total of six piezoelectric sensors are attached to the specimen in such a way that three are on the front and three on the back of specimen. A randomly oritented spackle pattern is applied on the region of interest, which is a segment of 25mm width on either side of the notch for acquiring and analyzing digital images which are recorded as a continuous video using a camera.

3 Results and discussion

This section describes the mechanical test findings of wedge-splitting experimental results, together with the AE and DIC data.

3.1 Results from AE and DIC

The load-CMOD curve obtained from experiments are presented in Figure 7. As expected, the peak load drops for specimens with higher a/d ratio. This is because of reduced intact ligament length for specimens with larger notch size. Figure 8 shows the splitting load, crack opening displacement (COD), the cumulative AE energy, AE events and crack length as a function of time. In this figure, the letters A, B, C, D, E, F, G, and I indicates the percentage of peak load in the post-peak region beginning from 100% (Peak load), 80%, 60%, 50%, 40%, 30%, 20%, 15%, 10% and 5%, respectively. The COD and crack lengths are obtained from the analysis of digital images. Furthermore, the crack opening contours from digital images are shown at different percentages of loading. From this figure, we can divide the complete load - time behaviour into four zones, I, II, III and IV based on the cumulative acoustic emission events and energy. A review of literature shows that the load - CMOD (CMOD as function of time) curve is generally classified into three zones- prepeak elastic region (similar to zone I), pre-peak nonlinear region (upto peak load) and the post-peak region. With the ability of acoustic emission data, we can classify the post-peak behaviour into two regions as explained below.

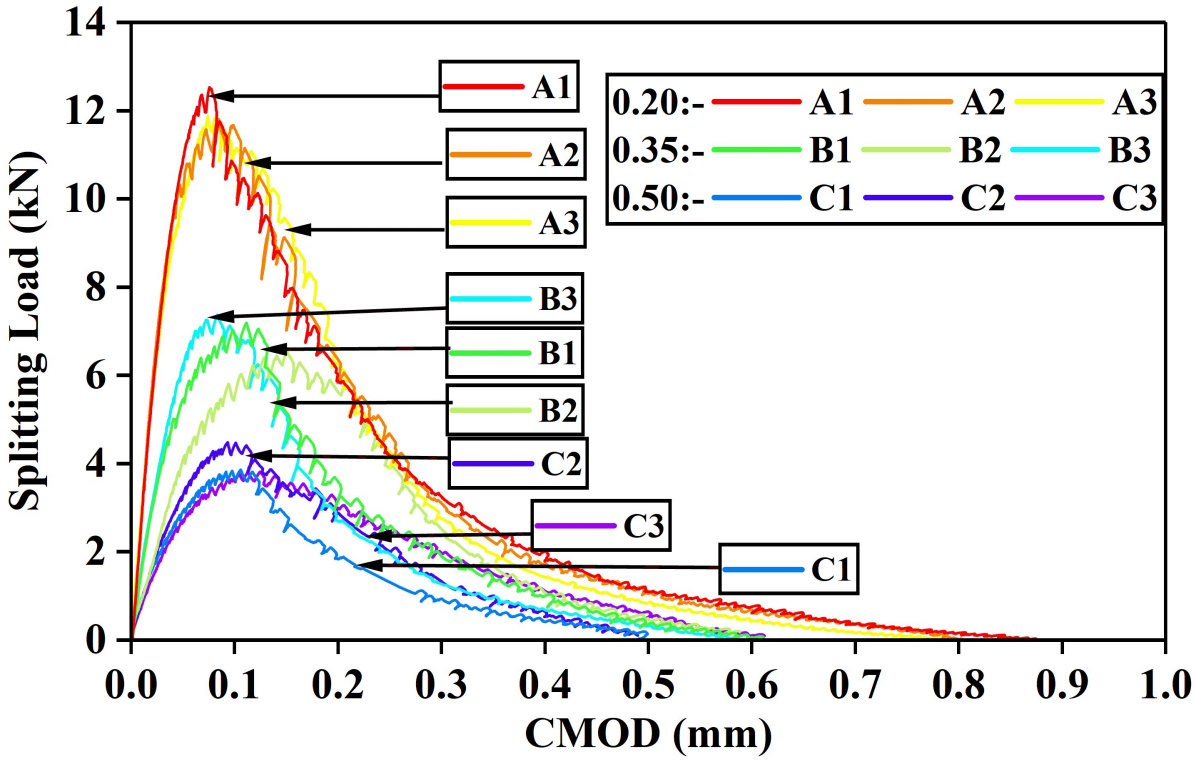

Figure 7: Load CMOD curves for specimens with differerent a/d

- Zone I- Elastic stage: This is initial stage, where in the load - time curve is linear upto about 80% of the peak load in the pre-peak region. Very few acoustic emission events occur in this region. The digital images also show no increase in the crack length.

- Zone II- Microcrack initiation stage: Microcracks begin to develop and grow as evident from the increase in AE events The AE energy remains constant while crack length starts to grow immediately after the peak load.

- Zone III- Steady crack growth stage: In this stage, the AE energy and events shows a steady increase. This indicates coalescence of microcracks and development of larger cracks, thereby releasing excess energy. The crack length also shows a steady increase.

- Zone IV- Unstable crack growth stage: The rate of increase of AE events, energy and crack length slows down in this stage and reaches their final value. The crack length increases and reach the end of ligament causing the specimen to break into two.

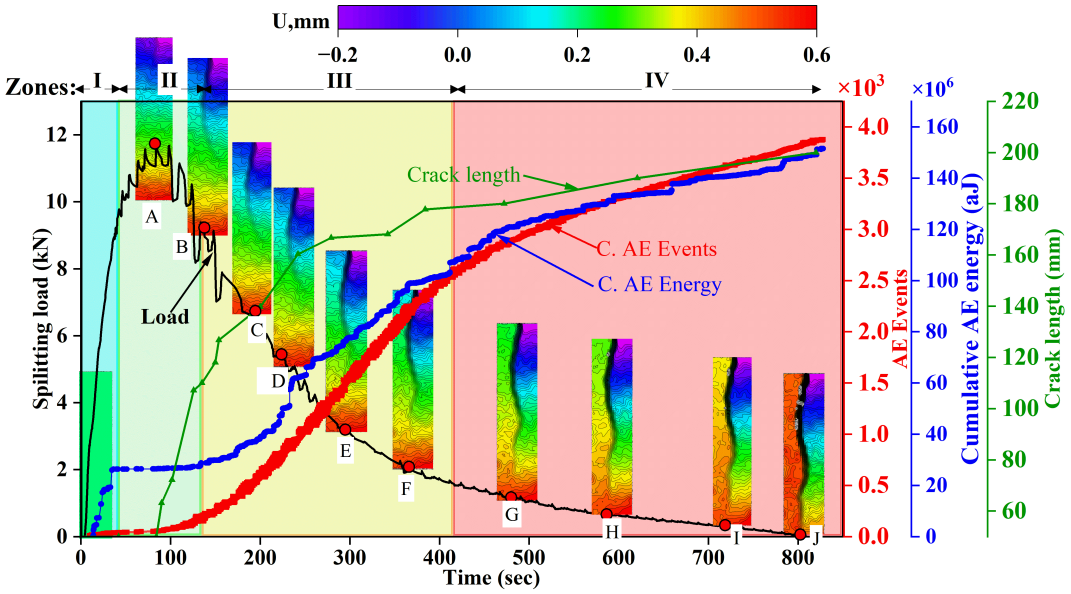

Figure 8: Load-CMOD curves with different zones based on AE Distribution

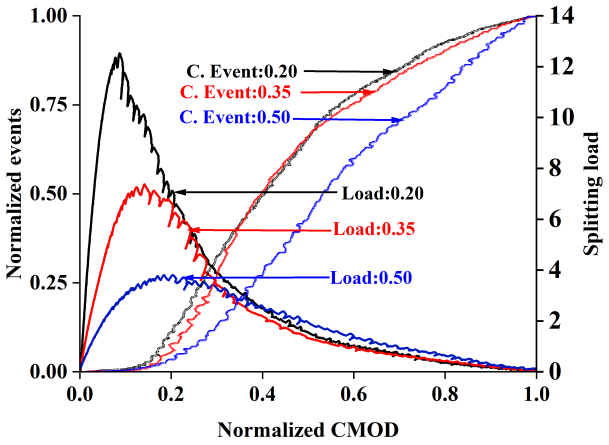

Figure 9: Load, normalised cumulative AE energy vs normalised CMOD

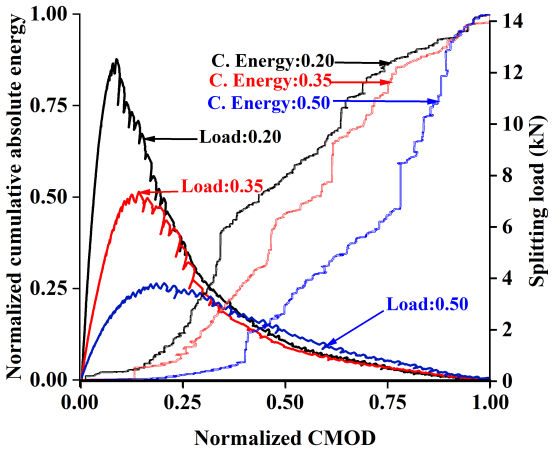

Figure 10: Load, normalised AE events vs normalised CMOD

Figure 9, shows the variation of normalised events and splitting load as a function of normalised CMOD for different notch sizes. It is seen that, the acoustic emission events do not differ much with the notch size and the rate of occurance of events are nearly the same for all notch sizes. Similar observation is seen in the Figure 10 for cumulative absolute energy, although there is a delay for larger notch size.

3.2 Fracture properties

From the experimental results, various fracture properties of plain concrete are evaluated and presented in the Table 2. The slope of initial linear portion of the load-CMOD plot gives the initial stiffness. The size-dependent fracture energy G_f is another fracture property given by the area under the load-COMD curve divided

Table 2: Properties from Load CMOD curve

Specimen textbfid	a/D	**Initial Stiffness**	**Peak Load**	**CMOD peak load**	**CMOD failure load**	**Size dependent fracture Energy**	**Stress intensity factor**
		kN/mm	kN	mm	mm	N/m	$MPa\sqrt{m}$
A1	0.20	302.4	12.53	0.076	0.87	137.29	1.40
A2	0.20	312.3	11.80	0.086	0.81	136.46	1.32
A3	0.20	282.5	11.88	0.074	0.80	131.33	1.32
Mean	**0.20**	**299.06**	**12.05**	**0.078**	**0.82**	**135.03**	**1.34**
SD (σ)	**0.20**	**12.39**	**0.24**	**0.005**	**0.032**	**2.63**	**0.04**
B1	0.35	124.00	7.19	0.111	0.61	92.52	1.08
B2	0.35	83.65	6.55	0.151	0.59	101.18	0.98
B3	0.35	130.43	7.37	0.083	0.59	84.02	1.10
Mean	**0.35**	**112.69**	**7.04**	**0.115**	**0.60**	**92.59**	**1.050**
SD (σ)	**0.35**	**20.70**	**0.35**	**0.003**	**0.01**	**7.00**	**0.052**
C1	0.50	54.61	3.86	0.106	0.49	61.90	0.84
C2	0.50	68.36	4.48	0.093	0.49	78.75	0.98
C3	0.50	57.39	3.82	0.125	0.61	89.06	0.83
Mean	**0.50**	**60.12**	**4.05**	**0.110**	**0.53**	**76.57**	**0.88**
SD (σ)	**0.50**	**5.93**	**0.30**	**0.010**	**0.06**	**11.19**	**0.07**

by the ligament area of the uncracked portion. The stress intensity factor is the crack characterising parameter which gives the state of stress at a critical location (crack-tip). The critical stress intensity factor, K_{IC} is calculated based on the RILEM recommendation [7]. K_{IC} is used to calculate the critical energy release rate, G_{IC}. Hence, although the fracture energy, G_f, is based on general behaviour, the critical stress intensity factor and critical energy release rate represent local parameters. Stress intensity factor for the wedge splitting configuration is given by Equation 2:

$$K_{IC}^{ini} = \frac{P_H}{BD^{1/2}} f(\alpha) \tag{2}$$

where $f(\alpha)$ is given by

$$f(\alpha) = \frac{3.675[1 - 0.12(\alpha - 0.45)]}{(1-\alpha)^{3/2}} \tag{3}$$

The following observations are made from this table:

- As a/D value increases, the initial stiffness and peak load of the specimen decreases.
- As a/D increases, CMOD at peak load also increases, however, a reverse tendency is observed in failure CMOD. The failure CMOD decreases with an increase in a/D. This is because of lower ligament length.

The size-dependent fracture energy and critical stress intensity factor K_{IC} are plotted against a/D in Figure 11. The parameters K_{IC} and G_{IC} are found to decrease with the increase of crack length. These parameters exhibits power-law variation as seen in the Figure 11.

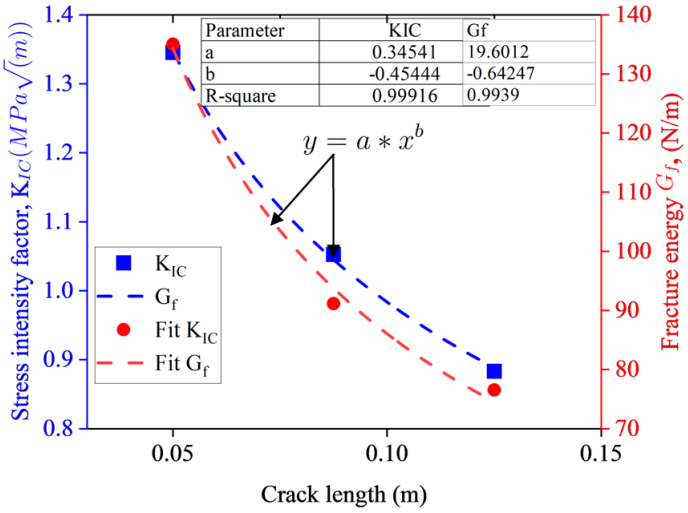

Figure 11: Variation of K and G with different notch sizes (a/D)

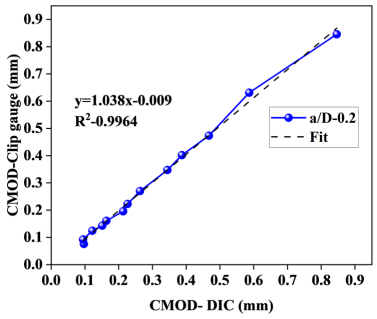

Figure 12: a/D-0.2

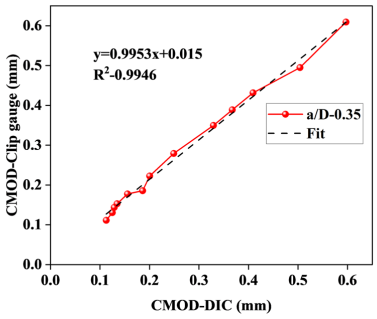

Figure 13: a/D-0.35

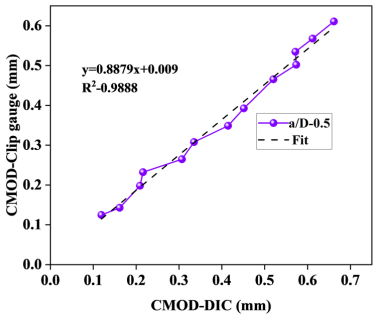

Figure 14: a/D-0.5

Figure 15: Comparision of CMOD with clip gauge and DIC analysis of WSP specimen for different a/D ratios

A virtual strain gauge is placed near the notch tip in image processing tool in order to measure the CTOD. CTOD is then converted to CMOD and compared with actual CMOD value from the experiments. In Figure 15, the variation between clip gauge CMOD and pseudo CMOD measurement from DIC is presented. All specimens show a similar trend with the slope varying between 41^0 to 46^0. Thus, the CMOD computed from DIC data shows good agreement with CMOD measured using clip gauge in the experiments.

4 Conclusions

In conclusion, wedge-splitting tests on plain concrete with various notch sizes were conducted to study the fracture behaviour under monotonically increasing crack opening with the aid of acoustic emission and digital image correlation methods. The following are the main conclusions of the study.

- The results show that increasing notch size leads to decrease in the size-dependent fracture energy and stress intensity factor of the concrete specimens.

The AE and DIC analyses provide detailed information on crack initiation and propagation, as well as deformation and strain fields on the surface.

- The AE data together with the load-CMOD characteristics have helped in identifying the fracture behaviour into four stages that include, elastic, micro crack initiation, steady crack growth and unstable crack growth stages.

- The AE events and energy do not show much variation with notch depth. This implies that the mechanisms of crack growth are similar for different notch size.

This study helps in understanding the effect of notch sizes on fracture behaviour of plain concrete and in designing specimen geometry for fatigue testing.

REFERENCES

[1] OE Gjorv, SI Srensen, and A Arnesen, 1977. Notch sensitivity and fracture toughness of concrete, *Cement and concrete research*; pp. 333-344.

[2] Bažant, Zdeněk P, 1984. Size Effect in Blunt Fracture: Concrete, Rock, Metal, *Journal of Engineering Mechanics*,110 (9), 518-535.

[3] H Cifuentes and BL Karihaloo, 2013. Determination of size-independent specific fracture energy of normal- and high-strength self-compacting concrete from wedge splitting tests, *Construction and Building Materials*; pp. 548-553.

[4] S Bhowmik and S Ray, 2019. An experimental approach for characterization of fracture process zone in concrete, *Engineering Fracture Mechanics*, 211 (00137944), 401-419.

[5] Keerthana. K and J. M. Chandra Kishen, 2020. Micromechanics of fracture and failure in concrete under monotonic and fatigue loadings, *Mechanics of Materials*, 148, 103490 .

[6] A Bakour and MB Ftima, 2020. Experimental investigations on the asymptotic fracture energy for large mass concrete specimens using wedge splitting test, *Construction and Building Materials*, 279, 122405.

[7] S Xu, Q Li, Y Wu, L Dong, Y Lyu, HW Reinhardt, CKY Leung, G Ruiz, Shailendra Kumar, Shaowei Hu. 2021. RILEM Standard: testing methods for determination of the double-K criterion for crack propagation in concrete using wedge-splitting tests and three-point bending beam tests, recommendation of RILEM TC265-TDK, *Materials and Structures*, 54, 1-11.

[8] A Bakour and MB Ftima, 2022. Investigation of fracture properties and size effects of mass concrete using wedge splitting tests on large specimens, *Engineering Fracture Mechanics*, 259, 108144.

[9] P Singh, Yogesh R, S Bhowmik, J. M. Chandra Kishen, 2023. Insights into the fracturing process of plain concrete under crack opening, *International Journal of Fracture*, 15732673.